

OFFICE OF NAVAL RESEARCH

Grant or Contract N0014-95-1-0302  
R&T Code 3132124

Technical Report No. 3

Direct and Photoinduced Absorption in Poly(p-pyridyl Vinylene):  
Morphological Control of Triplet Excitons and Polarons

by

S.W. Jessen, J.W. Blatchford, Y.Z. Wang, D.D. Gebler, L.-B. Lin, T.L. Gustafson, A.J.  
Epstein, T. Yuzawa, H. Hamaguchi, D.-K. Fu, M.J. Marsella, T.M. Swager and A.G.  
MacDiarmid

Prepared for publication in

Physical Review Letters

The Ohio State University  
Department of Physics  
Columbus, OH

March 1, 1996

Reproduction in whole in part is permitted for any purpose of the  
United States Government

This document has been approved for public release and sale;  
its distribution is unlimited.

This statement should also appear in item ten (10) of the Document Control Data  
DD Form 1473. Copies of the form available from cognizant or contract  
administrator.

19960314 052

DTIC QUALITY INSPECTED 1

# Direct and Photoinduced Absorption in Poly(*p*-pyridyl vinylene): Morphological Control of Triplet Excitons and Polarons

S. W. Jessen<sup>a</sup>, J. W. Blatchford<sup>a</sup>, Y. Z. Wang<sup>a</sup>, D. D. Gebler<sup>a</sup>, L.-B. Lin<sup>b</sup>, T.L. Gustafson<sup>b</sup>,  
and A. J. Epstein<sup>a,b</sup>

<sup>a</sup>*Department of Physics and* <sup>b</sup>*Department of Chemistry, The Ohio State University,  
Columbus, Ohio 43210-1106*

T. Yuzawa and H. Hamaguchi

*Molecular Spectroscopy Laboratory, Kanagawa Academy of Science and Technology,  
3-2-1 Sakato, Kawasaki 213, Japan*

D.-K. Fu, M. J. Marsella, T. M. Swager, and A. G. MacDiarmid

*Department of Chemistry, University of Pennsylvania,  
Philadelphia, Pennsylvania, 19104-6323*

## Abstract

Optical and photoinduced absorption (PA) studies of the polymer poly(*p*-pyridyl vinylene) (PPyV) are reported. Differences in the PA of powders and films of PPyV demonstrate that the relative stability of the photoexcited species (singlet and triplet excitons, polarons) varies with environment as a result of an enhanced intersystem crossing (ISC) route due to the presence of a nitrogen heteroatom in the backbone of the polymer chain. We conclude that triplet excitons and polarons are photocreated in powders and polarons are photocreated in films.

PACS numbers: 78.72.20.jv, 78.40.-q, 78.66.qn

Typeset using REVTeX

Upon photoexcitation or doping a conjugated polymer, the electronic excitations can self-localize via the electron-lattice interaction to form soliton or polaron states [1–3]. In addition, photoexcitation can produce metastable neutral excitations, as observed in organic molecular solids [4]. Earlier research focused on the photoexcited electronic states of degenerate ground state polymers such as polyacetylene [1] and the pernigraniline base form of polyaniline [5], for which the primary states are solitons and polarons, and nondegenerate ground state polymers such as polythiophene (PT) [1], for which polarons and bipolarons are central. Excitons are important in conjugated polymers which luminesce, such as poly(*p*-phenylene vinylene) (PPV) and poly(*p*-phenylene) (PPP). The radiative and nonradiative decay paths of the excited states in polymers such as PPV, PPP and their pyridine based analogues, poly(*p*-pyridine) (PPy) and PPyV are of particular interest, since these polymers have been used as the emitting layers in light emitting diodes (LEDs) [6–8] and other novel devices [9].

Recently, there has been controversy concerning the nature of the absorption peaks for PPV and its derivatives [10–16]. The exciton binding energy has been predicted to range between the values of 0 eV to  $\sim 1.0$  eV [10–16]. Another issue is whether one expects to see three or four absorption peaks for energies less than 7 eV [10,13]. Using a simple model based upon excitations in the phenylene monomer, Gartstein *et al.* [10] show that, as long as charge conjugation symmetry is not broken, one expects three absorption bands. Chandross *et al.* [13] use a modified Pariser-Parr-Pople model to show that four bands are expected in PPV.

The nature of the primary photoexcitations in PPV has been under considerable debate over the last few years. Photoinduced absorption (PA) studies on films of PPV reveal a strong triplet-triplet transition ( $T - T^*$ ), indicating that ISC from the singlet to triplet manifold may be one of the many possible nonradiative decay paths. Though bipolarons were reported [17] for disordered samples of PPV, they are not observed in more ordered samples [18].

PPyV is the pyridine based analogue of PPV (Fig. 1 inset). The addition of a nitrogen heteroatom within the ring introduces nonbonding ( $n, \pi^*$ ) states and breaks the charge con-

jugation symmetry of the polymer. Processibility of PPyV enables study of this polymer in solution, powder and film forms. Quantum chemical calculations on PPyV [19] demonstrate the role of the  $(n, \pi^*)$  states relative to the  $(\pi, \pi^*)$  states. These studies show that the lowest lying  $(n, \pi^*)^1$  state lies lower than the lowest  $(\pi, \pi^*)^1$  state for pyridine and bipyridine, inhibiting these molecules from fluorescing. The relative positions of the levels are reversed in PPyV, allowing this polymer to fluoresce. In addition, the relative locations of the  $(n, \pi^*)^1$  and  $(\pi, \pi^*)^3$  states can influence the photophysics of PPyV via enhanced ISC due to spin-orbit interaction [20]. Time resolved luminescence studies support these results [21].

In this Letter, we address the nature of the absorption and the photoexcitations on the ms time scale via photoinduced absorption (PA) studies for powder and film forms of PPyV. As predicted by models which incorporate broken charge conjugation symmetry [10] and Coulombic interaction [13], we observe four absorption features in PPyV below 7 eV. Depending upon the morphology and local order of the polymer sample, the nature of the dominant (millisecond) photoexcited state changes. Triplet exciton and polaron formation are observed in PPyV powders. Features attributed to polaron formation are reported for films of PPyV. We suggest that the differences in the two spectra are a result of differences in the amount of disorder. In particular, the presence of a nitrogen heteroatom in the polymer backbone introduces nonbonding  $(n, \pi^*)$  states which can alter triplet exciton production. The amount of mixing between the  $(n, \pi^*)$  and  $(\pi, \pi^*)$  states determine the extent to which there is enhanced triplet exciton production in powder and film forms of PPyV. In addition to reporting ms photoinduced infrared active vibrational (IRAV) modes, we report, for the first time in nondegenerate conjugated polymers, the observation of ns IRAV modes using a novel technique, which confirms the presence of free polarons in powders of PPyV at least as early as 20 ns.

The polymer samples were synthesized in powder form [22], mixed with KBr, and pressed into pellets for the optical measurements. Films were spin cast directly onto quartz substrates from solutions of the polymer in formic acid ( $\text{HCOOH}$ ). Optical measurements were

performed with a Perkin-Elmer Lambda 19 UV/VIS/NIR spectrometer for the direct absorbance and a SCINTAG Pad5 X-ray diffractometer for the X-ray diffraction measurements. The ms PA measurements were carried out using a homemade setup and are discussed elsewhere [23].

Details of the ns photoinduced IRAS system have been described elsewhere [24]. The global infrared source in a Hitachi I-3000 grating IR spectrometer was replaced by a JASCO MoSi<sub>2</sub> infrared source. Additional mirrors were added to the spectrometer, allowing the probe beam to be focused upon the sample. The thermocouple in the spectrometer was also replaced by either a photovoltaic (for ns time-resolved measurements) or photoconductive (for submicrosecond time range measurements) MCT detector. Optical pumping was performed with a Spectra-Physics TFR cw Q-switched Nd:YLF laser. Simultaneous data acquisition in both time and wavenumber domain was achieved with a digital oscilloscope.

Figure 1 presents the experimental absorption spectra for film (dashed) and powder (solid) samples of PPyV at 300 K, together with the absorption spectrum (dotted) calculated for a 4-ring oligomer. Four peaks are observed in the film spectrum, at 3.0 eV, 4.4 eV, 5.2 eV and 6.3 eV. For the calculation, the ground state geometry was optimized using MNDO-PM3. The absorption spectrum was calculated by including configuration interaction between single excitations. A Gaussian broadening was introduced. The quantum chemical calculations demonstrate two larger features with shoulders appearing on the low energy side of the higher energy feature. The calculated features agree with those observed in the film spectrum and are consistent with the prediction of models which include the presence of Coulomb interactions [13] and charge conjugation symmetry breaking [10]. Both the powder and film spectra are broad and featureless; however, the film spectrum has broader features and a more pronounced tail into the infrared, which has been contributed to aggregate formation [25].

The ms PA spectrum for powders and films of PPyV are shown in Figure 2. For the ms PA, we pumped with the 2.71 eV line of a cw Ar<sup>+</sup> laser at an incident intensity upon the sample of 150 mW/cm<sup>2</sup>. The pump beam was chopped at 15 Hz and the sample was

cooled to 80 K. For powder samples, there is a PA peak at 1.8 eV with a PA shoulder around 0.9 eV. The 1.9 eV signal is an artifact attributed to saturation of the sample with the probe beam due to the large cross section for triplet exciton absorption. The onset of photoinduced bleaching (PB) is observed at 2.5 eV. The quadrature signal in the powder samples reveals the shoulder to be a PA peak at 0.9 eV, as displayed in the left inset to Figure 2. PA peaks are seen at 1.0 eV and 1.7 eV for films of PPyV, with the onset of PB occurring at 2.3 eV. The ms PA signal of films, as displayed in Fig. 2, has been multiplied by a factor of 10. The lower energy onset of PB for films being consistent with the longer tail into the IR of the optical absorption. The right inset to Figure 2 shows the X-ray diffraction signal for powders (top) and films (bottom) of PPyV at 300 K. In both cases, the feature at  $13^\circ$  is attributed to the vacuum grease used to adhere the samples to the silicon substrate. Additionally, powders display one broad feature centered at  $25^\circ$ , while films have two broad features located at  $20^\circ$  and  $25^\circ$ , indicating different local order in the films.

Figure 3 shows the ms and time integrated ns (0 - 2000 ns) photoinduced IRAV modes for powders at 80 K and 300 K respectively. The ms photoinduced IRAV modes for films of PPyV are similar to the modes observed in the powder spectrum. For the ns spectrum, the 3.56 eV pump beam had an incident intensity of  $20 \mu\text{J}/\text{pulse}$  with a spot size of  $\sim 2$  mm diameter. Both spectra have photoinduced IRAV modes at  $1100 \text{ cm}^{-1}$ ,  $1160 \text{ cm}^{-1}$ ,  $1270 \text{ cm}^{-1}$ ,  $1360 \text{ cm}^{-1}$ ,  $1450 \text{ cm}^{-1}$  and  $1550 \text{ cm}^{-1}$ , though the first four modes are less pronounced in the ns regime. The inset shows the decay dynamics for the  $1270 \text{ cm}^{-1}$  peak. Similar decays are seen for the remaining modes with a power law dependence ( $\sim t^{-0.2}$ ).

Figure 4(a) shows the magnitude of the PA signal of PPyV as a function of the incident intensity for both powder and film samples. The maximum incident intensity ( $I_0$ ) was  $150 \text{ mW}/\text{cm}^2$  and the samples were held at a temperature of 80 K. The 1.8 eV peak ( $\circ$ ) in powders varies as  $\sim I$ , while the remaining features vary as  $\sim I^{0.5-0.6}$  for both the powder and film samples. The linear dependence with pump intensity indicates that the 1.8 eV peak decays monomolecularly, while the sublinear dependence of the remaining peaks indicate bimolecular decay. Thus, upon photocreation at least two types of photoexcited states are

present in PPyV on the ms time scale.

Figure 4(b) displays the chopper frequency dependence of all the peaks under the same experimental conditions as Fig. 3 ( $I_0 = 150 \text{ mW/cm}^2$ ,  $T = 80 \text{ K}$ ). The 1.8 eV peak ( $\circ$ ) has a weaker frequency dependence ( $\sim \omega^{-0.01}$  up to 300 Hz) than the 0.9 eV peak ( $\square$ ) and IRAV modes ( $\diamond$ ) ( $\sim \omega^{-0.4}$  for frequencies greater than 30 Hz) in powder samples. The film features ( $\triangle$ ) have similar frequency dependences ( $\sim \omega^{-0.4}$ ) to the 0.9 eV feature in powders. Further, from the 'knee' in the plot [26], we estimate the lifetime of the photoexcited state associated with the 1.8 eV peak to be  $\sim 1 \text{ ms}$ , while the lifetime associated with the remaining features is considerably longer and is estimated to be  $\sim 10 \text{ ms}$ .

Due to the linear dependence on pump beam intensity (monomolecular recombination) and relatively long lifetime ( $\sim 1 \text{ ms}$ ), we attribute the 1.8 eV PA signal of the powder form to the transition between triplet exciton states ( $T - T^*$ ). Photoluminescent detected magnetic resonance (PLDMR) studies indicate triplet exciton production in powders of PPyV [27]. Picosecond (ps) PA studies indicate a spectral response at 1 ns delay times which tracks the ms PA spectrum. Further, the long lived ps triplet signal is observed in dilute solutions at room temperature, indicating an intrachain phenomenon. Finally, the ps excitation profile at 1.9 eV tracks the PL, indicating direct conversion of singlet to triplet excitons [25].

The 0.9 eV feature is attributed to the lower energy transition associated with polarons. The strong  $T - T^*$  transition lies very close to the higher energy transition for polarons (as seen for films) and may obscure the weaker signal. The two PA features in PPyV films also are associated with polarons, as suggested by the similarities between these features and the low energy features in powders. The intensity and frequency dependence of the 0.9 eV feature in powders and films and the 1.7 eV feature in films indicates a long-lived state with sublinear intensity dependence. This is consistent with bimolecular recombination, as would be the case for polarons or bipolarons. Recent calculations [3] for oligomers of PT and PPP have suggested that the number of photoinduced transitions is two for polarons and one for bipolarons, in contrast to the earlier suggested three and two, respectively [2].

We observe a correlation with IRAV modes, indicating the photoexcited state is charged.

The ns photoinduced IRAV modes have similar power law dependence indicating polaron formation, as has been demonstrated for electronic features ( $> 0.4$  eV) in other conjugated polymers [28,29]. We have observed a strong mode in the ns spectrum at  $1270\text{ cm}^{-1}$  in polypyridine [27], which is strongly diminished in PPyV. We associate this mode with a C-N stretch within the aromatic unit [30]. The attenuation of this mode in PPyV is consistent with polaron formation centered primarily upon the vinylene unit, as proposed for PPV [11]. By summing the energies for the optical transitions between polaron levels [1,3], we obtain a predicted band gap energy of 3.8 eV, inconsistent with the measured absorption edge (onset of photoinduced bleaching) of 2.2 eV (Fig. 2). This supports that the lowest lying absorption feature is not the one electron bandgap, but an exciton absorption and that Coulomb correlations are very important for this class of materials.

Triplet excitons are observed in powders of PPyV and are not evident in films. A decrease in the production of triplet excitons or an increase in the production of polarons or both are possible explanations for the differences between powder and film PA. By comparing the photoinduced IRAV and photoinduced electronic features of powder and films, the volume density of polarons is nearly the same for both forms. Picosecond PA studies reveal smaller triplet exciton production in films as compared to that of powders of PPyV [25]. An enhanced ISC route may result in pyridine based polymers if a  $(n, \pi^*)$  state lies between the lowest  $(\pi, \pi^*)^1$  and  $(\pi, \pi^*)^3$  states [20]. Quantum chemical calculations on planar PPyV indicate that the lowest lying  $(n, \pi^*)$  states have energies greater than 4.0 eV. Therefore, enhancement of ISC is not expected to occur in the planar polymer; however, deviations from planarity result in substantial mixing of the  $(\pi, \pi^*)$  and  $(n, \pi^*)$  manifolds, leading to enhanced production of the triplets around the structural defect [25]. Powders are precipitated from a solvent in which they are insoluble. From the diffraction data, powders may have less structural order than films and thus are more likely to have an increased density of torsional defect sites. The polymer chains in PPyV films are probably more planar, since they are spin cast from a solution in which they are likely well extended. This would account for the enhanced ISC observed in the powders as compared with the films reported here.



In summary, the nature of the ms PA varies depending upon the method by which the sample is prepared. Powders are dominated by a large PA signal attributed to triplet excitons; whereas, films yield a PA signal attributed to polaron formation. The extent of enhanced triplet exciton production is suggested to be determined by the amount of mixing of the  $(n, \pi^*)^1$  and  $(\pi, \pi^*)^3$  states through torsional defects sites along the polymer chain and the local structural order.

This research was supported in part by the Office of Naval Research.

## REFERENCES

- [1] A. J. Heeger *et al.*, Rev. Mod. Phys. **60**, 781 (1988).
- [2] K. Fesser, A. R. Bishop and D. K. Campbell, Phys. Rev. B **27**, 4804 (1983).
- [3] Y. Furukawa, Synth. Met. **69**, 629 (1995).
- [4] J. B. Birks, *Organic Molecular Physics*, (J. Wiley and Sons, 1975).
- [5] J. M. Ginder and A. J. Epstein, Phys. Rev. B **41**, 10674 (1990).
- [6] D. D. C. Bradley *et al.*, Synth. Met. **41-43**, 3135 (1991).
- [7] G. Grem *et al.*, Adv. Mater. **4** 36 (1992).
- [8] D. D. Gebler *et al.*, J. Appl. Phys. **78**, 4264 (1995).
- [9] Y. Z. Wang *et al.*, Appl. Phys. Lett., *in press*.
- [10] Yu. N. Gartstein, M. J. Rice and E. M. Conwell, Phys. Rev. B **51**, 5546 (1995); M. J. Rice and Yu. N. Gartstein, Phys. Rev. Lett. **73**, 2504 (1994).
- [11] P. Gomes da Costa and E. M. Conwell, Phys. Rev. B **48**, 1993 (1993).
- [12] D. Beljonne *et al.*, J. Chem. Phys. **102**, 2042 (1995).
- [13] M. Chandross *et al.*, Phys. Rev. B **50**, 14702 (1994).
- [14] J. M. Leng *et al.*, Phys. Rev. Lett. **72**, 156 (1993).
- [15] S. Abe *et al.*, Phys. Rev. B **45**, 8264 (1992).
- [16] Z. G. Soos, S. Ramasesha and D. S. Galvão, Phys. Rev. Lett. **71**, 1609 (1993).
- [17] N. F. Colaneri *et al.*, Phys. Rev. B **42**, 11670 (1990).
- [18] K. Pichler *et al.*, J. Phys. Condens. Matter **5**, 7155 (1993).
- [19] J. W. Blatchford *et al.*, *to be published*.

- [20] M. A. El-Sayed, J. Chem. Phys. **38**, 2834 (1962).
- [21] L. B. Lin *et al.*, *to be published*.
- [22] M. J. Marsella, D.-K. Fu, and T. M. Swager, Adv. Mater. **7**, 145 (1995).
- [23] R. P. McCall *et al.*, Phys. Rev. B **41**, 5202 (1990).
- [24] T. Yuzawa *et al.*, Appl. Spect. **48**, 684 (1994).
- [25] J. W. Blatchford *et al.*, Phys. Rev. Lett., *in press*.
- [26] C. Botta *et al.*, Phys. Rev. B **48**, 14809 (1993).
- [27] S. W. Jessen *et al.*, *to be published*.
- [28] M. G. Roe *et al.*, Phys. Rev. B **40**, 4187 (1989).
- [29] G. S. Kanner and Z. V. Vardeny, Synth. Met. **49-50**, 611 (1989).
- [30] R. M. Silverstein and G. C. Bassler, *Spectrometric Identification of Organic Compounds*, (John Wiley and Sons, Inc., 1963), p. 67.

**Figure 1.** Optical Absorption of PPyV. Powder (solid), film (dashed) and calculated (dot) optical absorption of PPyV. The inset shows the schematic structure of PPyV.

**Figure 2.** PA spectrum of powders (solid) and films (dashed) of PPyV. PA is observed at 1.8 eV with a shoulder at 0.9 eV for powders. Films are multiplied by a factor of 10 and show PA peaks at 0.9 eV and 1.7 eV. The left inset shows the quadrature (out of phase) signal for powders. The right inset shows the X-ray diffraction signal for powders (top) and films (bottom) of PPyV.

**Figure 3.** Photoinduced IRAV modes of PPyV. The time integrated ns IRAV (bottom) and the ms IRAV (top) modes are shown. The inset shows the decay kinematics of the ns IRAV modes.

**Figure 4.** Parameter Dependence of PPyV. a) Intensity dependence of the 0.9 eV in powders ( $\square$ ), 1.7 eV in films ( $\triangle$ ), 1.8 eV in powders ( $\circ$ ), and IRAV ( $\diamond$ ) features. b) Frequency dependence of the 0.9 eV, 1.7 eV (film), 1.8 eV (powders), and IRAV features.

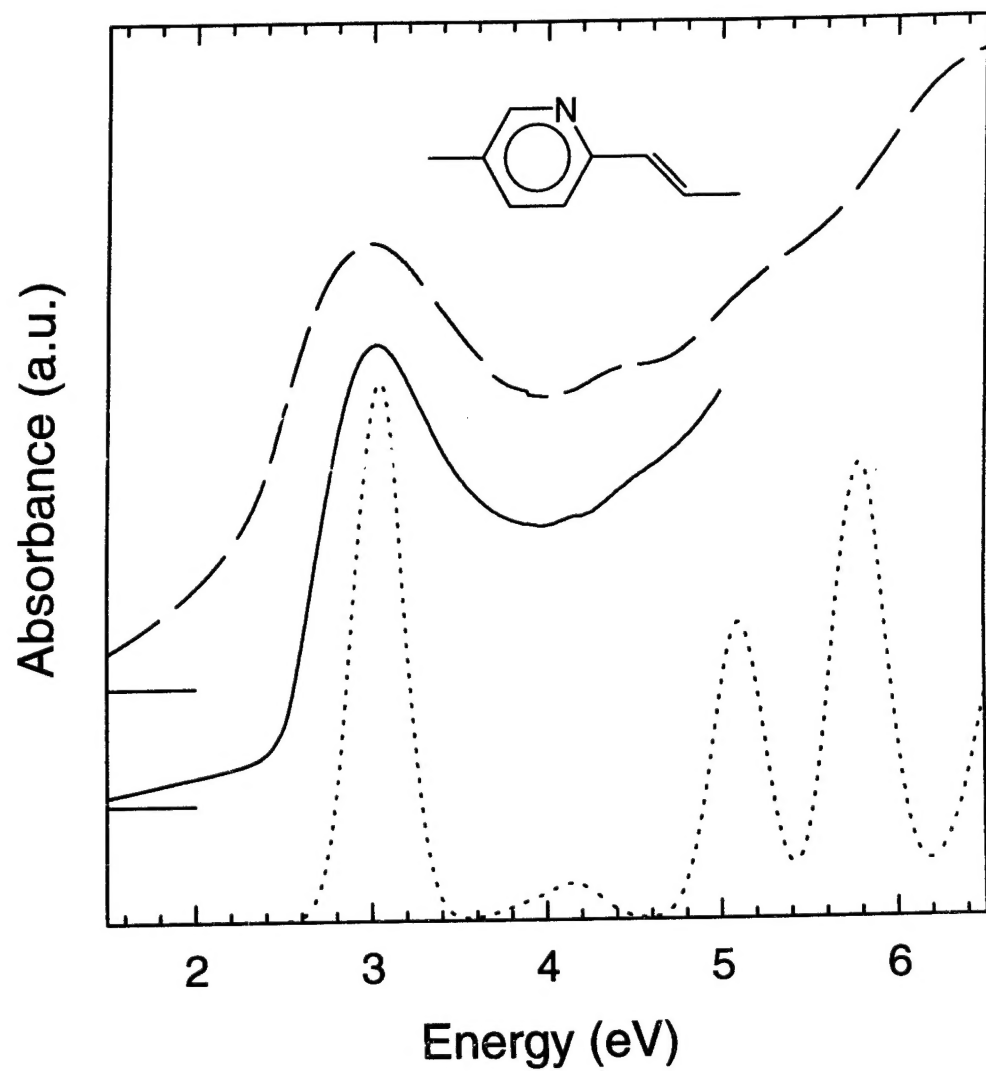


**Figure 1, Jessen *et al.***

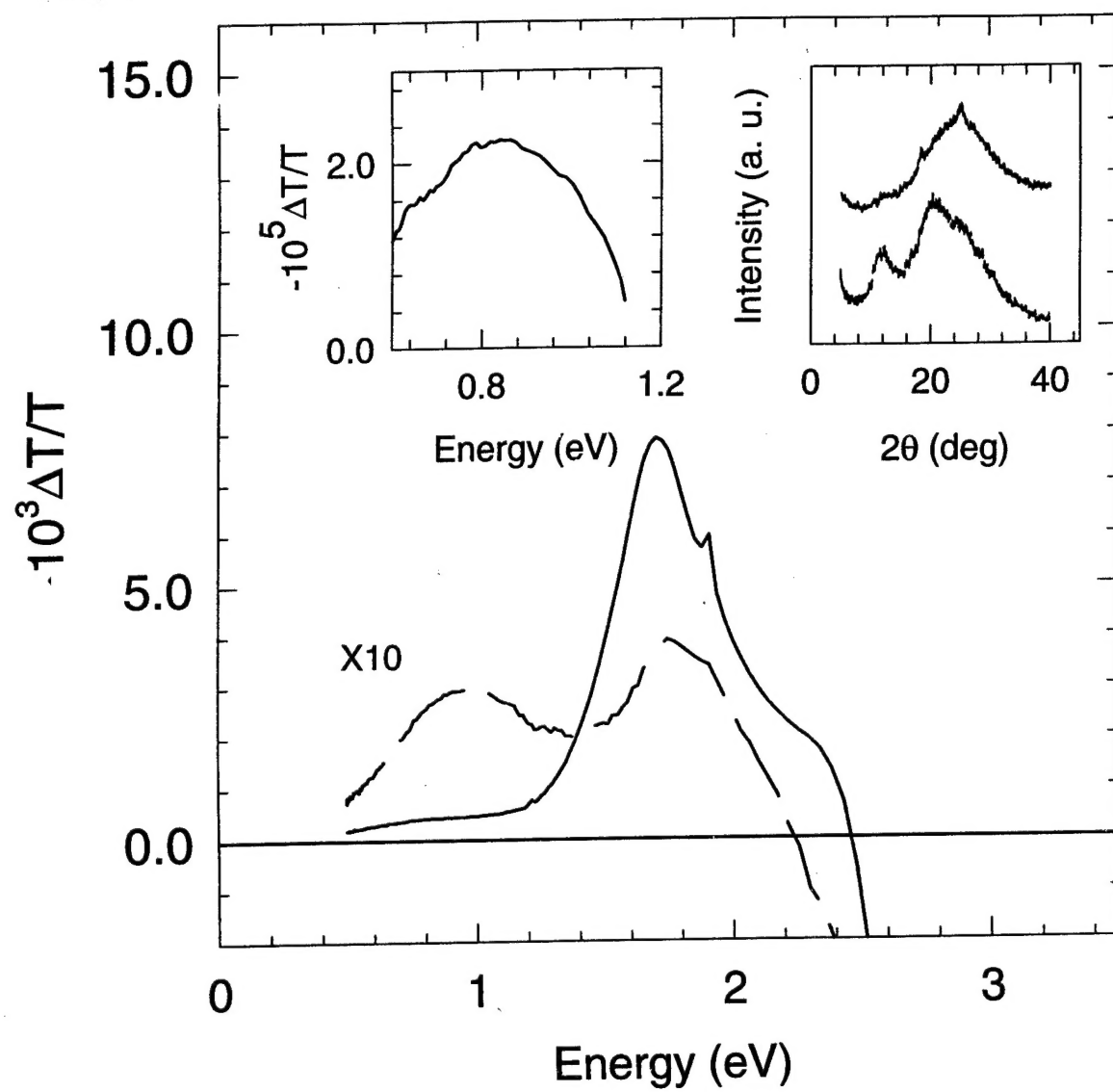


**Figure 2, Jessen *et al.***

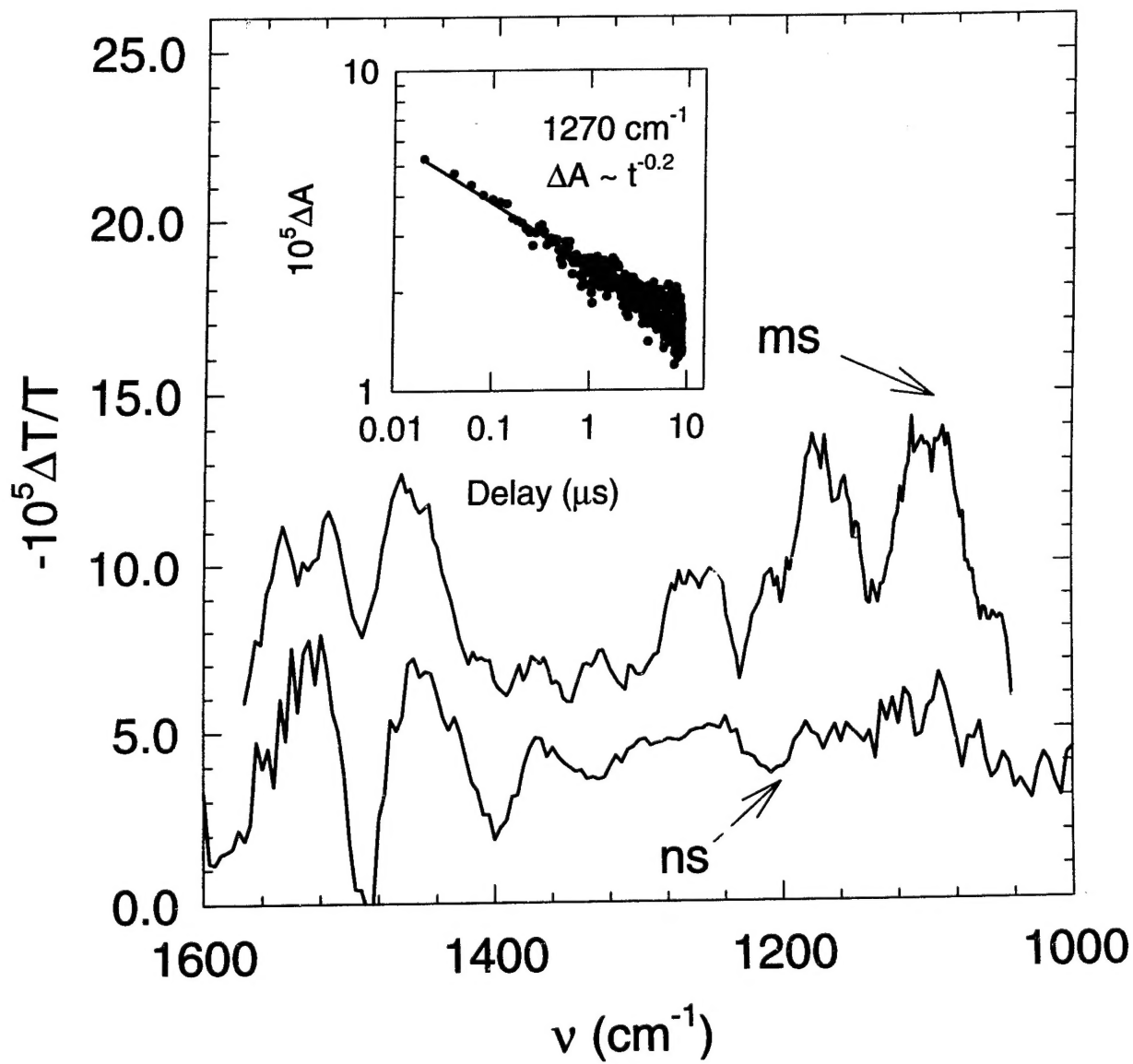


**Figure 3, Jessen *et al.***

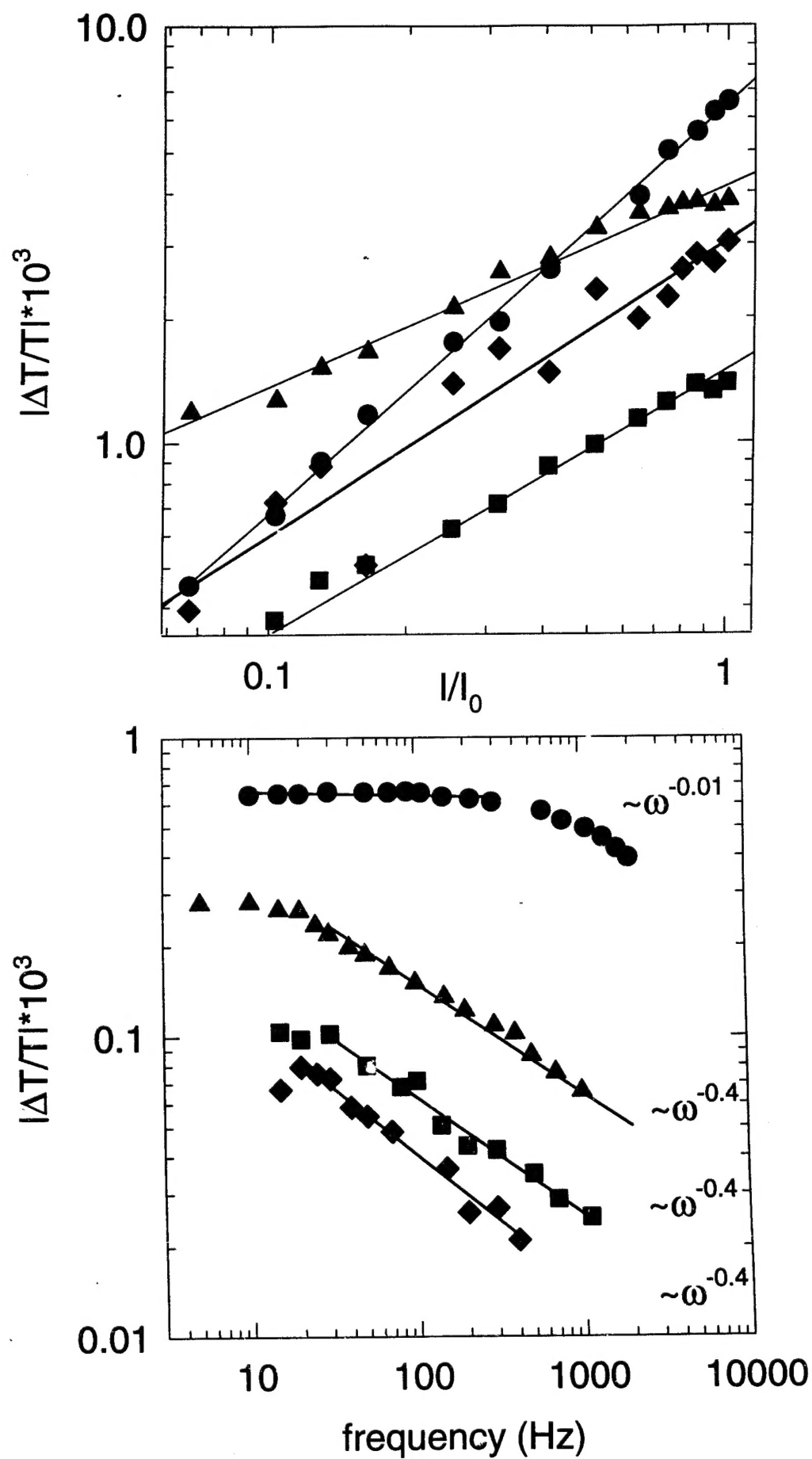


Figure 4, Jessen *et al.*